

Slovenská technická univerzita v Bratislave
Stavebná fakulta

RNDr. Ing. Matúš Tibenský

Autoreferát dizertačnej práce

**Usage of the gradient schemes for
numerical solution of non-linear parabolic equations**

na získanie akademického titulu *philosophiae doctor (PhD.)*
v doktorandskom študijnom programe
9.1.9 Aplikovaná matematika

Bratislava 2018

Dizertačná práca bola vypracovaná v dennej forme doktorandského štúdia na Katedre matematiky a deskriptívnej geometrie SvF STU v Bratislave.

Predkladateľ: RNDr. Ing. Matúš Tibenský
Katedra matematiky a deskriptívnej geometrie
SvF STU, Bratislava

Školiteľ: Doc. RNDr. Angela Handlovičová, PhD.
Katedra matematiky a deskriptívnej geometrie
SvF STU, Bratislava

Oponenti: Prof. RNDr. Igor Bock, PhD.
Ústav informatiky a matematiky
FEI STU, Bratislava

Prof. RNDr. Ján Filo, CsC.
Katedra matematickej analýzy a numerickej matematiky
FMFI UK, Bratislava

Doc. RNDr. Peter Frolkovič, PhD.
Katedra matematiky a deskriptívnej geometrie
SvF STU, Bratislava

Autoreferát bol rozoslaný dňa

Obhajoba dizertačnej práce sa koná dňa o hod. na Katedre matematiky a deskriptívnej geometrie SvF STU v Bratislave, Radlinského 11.

prof. Ing. Stanislav Unčík, PhD.
dekan Stavebnej fakulty

Abstract

In this thesis we deal with numerical methods used for solving non-linear time dependent partial differential equations, where the biggest challenge is numerical approximation of the gradient. We apply this approach in two fields, therefore is the thesis divided into two parts.

In the first one we present finite volume scheme based on the EHM (Eymard-Handlovicova-Mikula) approach and apply it in the image segmentation process. We introduce new model, so-called regularised Riemannian mean curvature flow equation. For this new model we prove the necessary theoretical aspects as uniqueness of the numerical solution, stability estimates for the numerical solution and the convergence of the numerical scheme to the solution. Regularised Riemannian mean curvature flow equation is tested on the benchmark examples to prove its suitability. In the end of the section two different approaches of the approximation of the non-linear smoothing term are discussed and compared.

The second part of the thesis is dedicated to the introduction of the discrete duality finite volume (DDFV) method and the application of this method for modelling of the development of the financial derivatives' price in time. So-called Heston model and its regularized version are studied. For the regularised model the stability estimates on the numerical solution and the convergence of the numerical scheme to the solution are proven. The last part is dedicated to the numerical experiments for the DDFV method for the regularised Heston model.

Keywords: finite volume method, level set, image segmentation, regularised Riemannian mean curvature flow equation, DDFV, financial derivatives pricing, regularised Heston model

Abstrakt

V tejto práci sa zaoberáme numerickými metódami na riešenie nelineárnych časovo závislých parciálnych diferenciálnych rovníc, kde hlavnou výzvou je aproximácia gradientu. Tento prístup aplikujeme v dvoch oblastiach, preto je práca rozdelená na dve časti.

V prvej časti prezentujeme metódu konečných objemov založenú na EHM (Eymard-Handlovičová-Mikula) prístupe a aplikujeme ju v procese segmentácie obrazu. Zavedieme nový model, takzvanú regularizovanú level set rovnicu s riemannovskou krivosťou. Pre tento model sme dokázali potrebné teoretické vlastnosti ako jedinečnosť numerického riešenia, stabilné odhady na numerické riešenie a konvergencia numerickej schémy k riešeniu. Regularizovaná level set rovnica s riemannovskou krivosťou je testovaná na príkladoch, aby bola dokázaná jej vhodnosť. Na konci sekcie su diskutované a porovnané dva rozdielne prístupy k aproximácii nelineárneho zhladzovacieho člena.

Druhá sekcia práce je venovaná uvedeniu diskkrétnej duálnej metódy konečných objemov (DDFV) a použitiu tejto metódy na modelovanie vývoja ceny finančných derivátov v čase. Študovaný je takzvaný Hestonov model a jeho regularizovaná verzia. Pre regularizovaný model sú dokázané stabilné odhady na numerické riešenie a konvergencia numerickej schémy k riešeniu. Posledná časť je vyhradená numerickým experimentom DDFV schémy pre regularizovaný Hestonov model.

Keywords: metóda konečných objemov, level set, segmentácia obrazu, regularizovaná level set rovnica s riemannovskou krivosťou, DDFV, oceňovanie finančných derivátov, regularizovaný Hestonov model

Contents

1	Introduction	3
2	Gradient Schemes in Image Segmentation Problems	5
2.1	Mathematical models and numerical method in image segmentation	5
2.2	Regularised Riemannian mean curvature flow equation	7
2.3	Numerical analysis of regularised Riemannian mean curvature flow model	9
2.4	Numerical experiments in image segmentation	10
3	Gradient Schemes in Financial Derivatives Pricing Problems	12
3.1	Mathematical models and numerical method in financial mathematics	12
3.2	Regularised Heston model	13
3.3	Numerical analysis of regularised Heston model	15
3.4	Numerical experiments in financial derivatives pricing	15
	References	18

Chapter 1

Introduction

The purpose of the thesis is to study problems in mathematical modelling that could be described by parabolic partial differential equations and to develop tools to solve these problems. As the studied problems are complex the describing equations are complicated and the corresponding initial-boundary problems have to be solved numerically.

From the wide range of the numerical methods we chose so-called Gradient Discretisation Method (GDM) approach based ones. Per his name, GDM approach handles with the numerical approximation of the gradient as this is the main challenge in our models - how to approximate the gradient of the solution.

The main publication describing the GDM is, for us, [8] from authors Droniou, Eymard, Gallouet, Guichard and Herbin, where the linear and non-linear cases for elliptic and parabolic problems are studied and necessary analysis tools are developed.

A numerical method obviously starts from selecting a finite number of degrees of freedom describing the finite dimensional space in which the approximate solution is sought. Per [8] $X_{\mathcal{D}}$ is meant to be finite dimensional space (\mathcal{D} for "discretisation"). The two linear operators $\Pi_{\mathcal{D}}$ and $\nabla_{\mathcal{D}}$ which respectively reconstruct, from the degrees of freedom, a function on Ω and its "gradient", are such that

$$\Pi_{\mathcal{D}} : X_{\mathcal{D}} \rightarrow L^2(\Omega), \quad \nabla_{\mathcal{D}} : X_{\mathcal{D}} \rightarrow L^2(\Omega)^d, \quad (1.1)$$

where d is dimension of Ω . In other words, the discretisation \mathcal{D} in GDM approach contains at least three following discrete entities:

- a discrete space of unknowns $X_{\mathcal{D}}$ - the values at the nodes of the mesh,
- a function reconstruction operator $\Pi_{\mathcal{D}}$ - transforms an element of $X_{\mathcal{D}}$ into a function defined a.e. on the physical domain Ω ,
- an approximate gradient reconstruction $\nabla_{\mathcal{D}}$ - builds a vector-valued function (discrete gradient) defined a.e. on Ω from the discrete unknowns.

Then the type of problems we are interested in (searching for the weak solutions of non-linear parabolic partial differential equations) could be turned to the problem of finding function $u_{\mathcal{D}} \in X_{\mathcal{D}}$ such that for all $v_{\mathcal{D}} \in X_{\mathcal{D}}$ holds weak formulation of the problem with discrete reconstruction operators defined above.

We have been speaking only about space discretisation, but there are various approaches to the time discretisation as well. Usually we can distinguish two main ones - explicit and implicit. The combination of these two is an option as well. The explicit approach is the simpler one as the state of a system at a later time is calculated from the state of the system at the current time. In other words if $U(t)$ is the state of the system at the time t and δt is a small time step we can write $U(t+\delta t) = f(U(t))$ with some function f . The main usual disadvantage of the explicit numerical methods is that there has to be restriction on the time and space step relation prescribed. On the other hand with the

implicit approach the solution is found by solving an equation involving both the current state of the system and the later one. In mathematical formulation equation $g(U(t), U(t + \delta t)) = 0$ has to be solved to find $U(t + \delta t)$.

From all methods that are described by GDM approach we are taking two - Finite Volume Method (FVM) and Discrete Duality Finite Volume method (DDFV). They are applied in the completely different fields of applied mathematics, therefore is the thesis divided into two parts, each is dedicated to the one numerical method and its application. From the time discretisation perspective in the first part of the thesis there is a semi-implicit method used, where the non-linear terms are taken from previous time step and the linear terms from the current one, so the system of the linear equations has to be solved. In the second part we are using fully implicit scheme as the problem prescribing equation is linear, so we are solving system of linear equations here as well.

Structure of both dissertation thesis parts is basically the same - introduction to the problematic (used mathematical models and numerical method), definition of the studied problem and appropriate numerical scheme, theoretical analysis of the defined numerical scheme and numerical experiments.

The FVM is applied in the field of the image processing, concretely in the image segmentation. Mathematical models based on time dependent partial differential equations used to deal with image processing and image segmentation problems are stated to introduce the studied problematic to the reader. As the next step we state the so-called **regularised Riemannian mean curvature flow equation**, the problem we are studying in the first part of the thesis, and the semi-implicit FVM approach based numerical scheme to solve this problem arising in objects segmentation and missing boundaries competition. The problem is studied from theoretical perspective and the uniqueness of the solution and convergence of the numerical scheme is proven, and from experimental perspective, when is the method tested on the benchmark examples to prove its robustness and suitability and different approaches to the non-linear smoothing term approximation are discussed and compared visually and numerically.

Second part of the thesis is dedicated to the financial derivatives pricing. Various models based on PDEs with relevant challenges are discussed, the appropriate numerical method, the DDFV, is stated and the application of this method in financial mathematics is shown. In the middle of our interest lies the so-called **regularised Heston model** and fully implicit DDFV numerical scheme for this model. In analogy to the first part of the thesis next two sections are dedicated to the theoretical and numerical study of the numerical scheme. The L_∞ stability of the scheme is proven, which leads to the proof of the DDFV scheme convergence, the main theoretical result of the second part of the thesis. In the numerical experiments for the regularised Heston model we pay attention especially to the role and impact of the regularisation parameter on the model results.

Chapter 2

Gradient Schemes in Image Segmentation Problems

One can find various approaches used in the image processing based on the different mathematical models, for instance on statistical analysis, graph theory, Fourier transformation or histograms of the image intensity. These approaches we are not interested in. We do not cover the approach based on the neural networks and machine learning as well, because this part of our work is dedicated to the usage of the partial differential equations in the image processing problems, especially in the image segmentation.

2.1 Mathematical models and numerical method in image segmentation

One of the main challenges we have to deal with in the image processing is noise. Pictures are often noisy, so they have to be de-noised before other analyses can be done - either extracting crucial information from the images or building models based on the images.

There are two main models of the noise used in the image processing - additive type of noise and salt and pepper type. Examples one can find in [11], [12] and [21].

The very simple model used for pictures de-noising is the one based on the heat equation, which is actually the convolution of the image density function with the Gaussian kernel. As the heat equation is linear PDE this is called linear filtration and it smooths the whole image evenly.

There are plenty of generalizations of the image filtration to the non-linear form. We will use, in some sense, two of them. One, proposed by Perona and Malik in 1987 (see [25] and [26]) is represented by so-called Perona-Malik equation:

$$\frac{\partial u(x, t)}{\partial t} = \nabla \cdot (g(|\nabla u|)\nabla u), \quad (2.1)$$

where the function g , edge detector, has following properties: $g(0) = 1$, $g(s) > 0$, $g(s) \rightarrow 0$ for $s \rightarrow \infty$ and $g'(s) < 0$ (g is decreasing function). Function g determinates the power of the smoothing and will be used in our model as well.

The second approach of the non-linear image filtration we are incorporating to our model is based on the idea of the curvature driven equations. The point is that the borders of the objects on the pictures are taken as the curves. Then we let these curves develop by their curvature. The assumption is that noise has very small radius compared to the actual objects, so after short time it will disappear and the borders of the objects will not change much. The point of the curvature driven methods is that borders of objects are represented as curves in 2D and as surfaces in 3D.

In the level set approach are these curves taken as isolines of the level set function (and surfaces as isosurfaces), so we have to monitor development of the set $u(x, t) = c$ for $\forall x \in \Omega$ and $\forall t \in [0, T]$, see

[24]. Indeed, following condition has to be fulfilled:

$$0 = \frac{d}{dt}(u(x(t), t)) = \frac{\partial u}{\partial t} + \nabla u \cdot \dot{x}. \quad (2.2)$$

Once we consider the curvature driven movement, when $\dot{x} = -\nabla \cdot \left(\frac{\nabla u}{|\nabla u|} \right) \frac{\nabla u}{|\nabla u|}$ the equation (2.2) moves to the form:

$$\frac{\partial u}{\partial t} - \nabla \cdot \left(\frac{\nabla u}{|\nabla u|} \right) \frac{\nabla u}{|\nabla u|} = \frac{\partial u}{\partial t} - |\nabla u| \nabla \cdot \left(\frac{\nabla u}{|\nabla u|} \right) = 0. \quad (2.3)$$

This equation is called level set equation (see [24]) usually used in the regularised form:

$$u_t = f(|\nabla u|) \nabla \cdot \left(\frac{\nabla u}{f(|\nabla u|)} \right), \quad (2.4)$$

where $f(s) = \sqrt{s^2 + \varepsilon^2}$ for $\varepsilon > 0$ sufficient small is called Evans-Spruck regularisation (see [9]) and it is used to prevent the zero denominators in the numerical scheme (when the gradient of the function u is zero). In our model we are using its generalised form.

In opposite to the image de-noising process the point and goal of the segmentation process is to divide the picture into alike groups of pixels called regions, to mark pixels of the object we are interested in or to add a border to the object where it is missing. The purpose of the segmentation is that sometimes we prefer picture to be divided into parts, simplified and better analysable.

Idea of the segmentation algorithm derivation is analogical to the ideas for problems of image processing presented above. So we can state analogy of the equation (2.4) in the image segmentation, so-called subjective surfaces equation (see [7]):

$$u_t = f(|\nabla u|) \nabla \cdot \left(g(|\nabla I^0|) \frac{\nabla u}{f(|\nabla u|)} \right). \quad (2.5)$$

We are using the finite volume method (FVM) to handle with the challenges stated above numerically. The FVM is discretisation method appropriate and therefore used for problems connected with the conservation laws. In general the conservation laws describe preservation of the quantity modelled by the function $q(x, t)$ that could be mass or energy and in our case it is the segmentation function. For more complex introduction to the finite volume method see our main publication regarding this theme - [10] from authors Eymard, Gallouet and Herbin.

As mentioned in the Introduction very important step in the numerical solution of PDEs is the discretisation of the domain Ω . For the FVM method it is the division of the domain into so-called control volumes. The unknown function, solution of the problem, is then approximated by the numerical solution, which is piecewise constant function in the FVM approach.

In addition for the FVM the crucial role in the numerical scheme compiling play the flows through the borders of the control volumes - on the border of the domain they are given by the boundary condition and inside of the domain they are linked by the conservation laws. Flow from the control volume p to the control volume q is equal to the flow from the control volume q to the control volume p with opposite sign:

$$\vec{F}_{p \rightarrow q} = -\vec{F}_{q \rightarrow p}. \quad (2.6)$$

We state two semi-implicit numerical schemes used in the image processing based on the finite volume method in the thesis - HMS (Handlovicova-Mikula-Sgallarri) scheme, see [16], and EHM (Eymard-Handlovicova-Mikula) scheme, see [12] or [13].

The difference between these two methods is in the gradient approximation principle on the borders of the control volume. We use the EHM approach, where is the gradient approximated locally on the given control volume by the so-called diamond cell method, see [23].

One can take a look on the Figure 2.1 taken from Manzini, see [2] or [4], to see the principle of the diamond cell method:

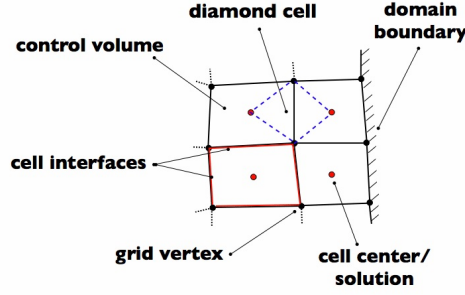


Figure 2.1: Finite volume method principle.

2.2 Regularised Riemannian mean curvature flow equation

Our goal is to study following non-linear parabolic equation arising in the image segmentation and the edge detection and to find numerical scheme for solving it:

$$u_t - f_1(|\nabla u|)\nabla \cdot \left(g(|\nabla G_S * I^0|) \frac{\nabla u}{f(|\nabla u|)} \right) = r, \quad a.e. (x, t) \in \Omega \times (0, T), \quad (2.7)$$

where $u(x, t)$ is an unknown (segmentation) function defined in $Q_T \equiv \Omega \times [0, T]$, where Ω is a finite connected open subset of \mathbb{R}^d , $d \in \mathbb{N}$, $[0, T]$ is a time interval and I^0 is a given image, typically on this image is an object we want to segment.

We consider zero Dirichlet boundary condition

$$u = 0, \quad a.e. (x, t) \in \partial\Omega \times [0, T] \quad (2.8)$$

and initial condition

$$u(x, 0) = u_0(x), \quad a.e. x \in \Omega. \quad (2.9)$$

Assumptions on the data in (2.7)-(2.8)-(2.9) can be summarized to the following hypothesis, we denote it as Hypothesis (H):

Hypothesis H

- (H1) Ω is a finite connected open subset of \mathbb{R}^d , $d \in \mathbb{N}$, with boundary $\partial\Omega$ defined by a finite union of subsets of hyperplanes of \mathbb{R}^d ,
- (H2) $u_0 \in L^\infty(\Omega)$,
- (H3) $r \in L^2(\Omega \times (0, T))$ for all $T > 0$,
- (H4) $f \in C^0(\mathbb{R}_+; [a, b])$ is a regularisation - Lipschitz continuous (non-strictly) increasing function, such that the function $x \mapsto x/f(x)$ is strictly increasing on \mathbb{R}_+ . For practical application we are using $f(s) = \min\{\sqrt{s^2 + a^2}, b\}$, where a and b are given positive parameters, $a \leq b$,
- (H5) $f_1 \in C^0(\mathbb{R}_+; [a_1, b_1])$, in general $a_1 \neq a$, $b_1 \neq b$, but for now in our model we, just for the sake of simplicity, consider the case $a_1 = a$ and $b_1 = b$,
- (H6) $g \in C^0(\mathbb{R}_+; [0, 1])$ is decreasing function of Perona-Malik type, $g(0) = 1$, $g(s) \rightarrow 0$ for $s \rightarrow \infty$. For practical numerical computation we use $g(s) = \frac{1}{1+Ks^2}$, where K is a constant of sensitivity of function g and we choose it,
- (H7) $G_S \in C^\infty(\mathbb{R}^d)$ is a smoothing kernel (Gauss function), with width of the convolution mask S and such that $\int_{\mathbb{R}^d} G_S(x)dx = 1$, $\int_{\mathbb{R}^d} |G_S|dx \leq C_S, C_S \in \mathbb{R}$, $G_S(x) \rightarrow \delta_x$ for $S \rightarrow 0$, where δ_x

is Dirac measure at point x and

$$(\nabla G_S * I^0)(x) = \int_{\mathbb{R}^d} \nabla G_S(x - \xi) \tilde{I}^0(\xi) d\xi, \quad (2.10)$$

where \tilde{I}^0 is extension of image I^0 to \mathbb{R}^d given by periodic reflection through boundary of Ω ,

- (H8) initial image I^0 is such that $I^0 \in L^\infty(\Omega)$.

Definition 2.1 (Weak solution of (2.7)-(2.8)-(2.9)) Under the Hypothesis (H), we say that u is a weak solution of (2.7)-(2.8)-(2.9) if, for all $T > 0$,

1. $u \in L^2(0, T; H_0^1(\Omega))$ and $u_t \in L^2(\Omega \times (0, T))$ (hence $u \in C^0(0, T; L^2(\Omega))$).
2. $u(\cdot, 0) = u_0$.
3. Following holds

$$\begin{aligned} \int_0^T \int_{\Omega} \left(\frac{u_t(x, t)v(x, t)}{f_1(|\nabla u(x, t)|)} + g(|\nabla G_S * I^0|) \frac{\nabla u(x, t) \cdot \nabla v(x, t)}{f(|\nabla u(x, t)|)} \right) dx dt = \\ = \int_0^T \int_{\Omega} \frac{r(x, t)v(x, t)}{f_1(|\nabla u(x, t)|)} dx dt, \forall v \in L^2(0, T; H_0^1(\Omega)). \end{aligned} \quad (2.11)$$

The space discretisation of the domain Ω is the triplet $\mathcal{D} = (\mathcal{M}, \mathcal{E}, \mathcal{P})$, where the symbol \mathcal{M} represents the so-called control volumes, \mathcal{E} is the set of the mesh edges and \mathcal{P} are points, there is one point in every control volume. For the time discretisation we are using the semi-implicit approach - the non-linear terms are taken explicitly and the linear terms implicitly.

The discrete solution of the problem is piecewise constant function in space and in time and is defined as

$$u_p^n = u(x_p, t) \quad (2.12)$$

for $t \in [n\tau, (n+1)\tau]$, $n = 1, \dots, N_T + 1$ and $\forall p \in \mathcal{M}$ and norm of its gradient is given by

$$N_p(u)^2 = \frac{1}{|p|} \sum_{\sigma \in \mathcal{E}_p} \frac{|\sigma|}{d_{p\sigma}} (u_\sigma - u_p)^2, \quad \forall p \in \mathcal{M}. \quad (2.13)$$

For the term g_D^S , approximation of the non-linear smoothing term, we introduce two possible approaches - **(APR1)**:

$$g_\sigma^S := g^S(x_\sigma) = g(|\int_{\mathbb{R}^d} \nabla G_S(x_\sigma - \xi) \tilde{I}^0(\xi) d\xi|) \quad (2.14)$$

and **(APR2)**:

$$g_p^S := g^S(x_p) = g(|\int_{\mathbb{R}^d} \nabla G_S(x_p - \xi) \tilde{I}^0(\xi) d\xi|). \quad (2.15)$$

In the first case is the convolution of the initial image with the Gaussian kernel done on the edge of the control volume, where it should be done as one can see in the scheme (2.20). For the second approach it is done in the point inside of the control volume, therefore there is an error included. Quantification of this error is the task we are solving in the numerical section of the first part of the thesis.

Under the above notations is the semi-implicit scheme for the problem (2.7)-(2.8)-(2.9) defined by

$$u_p^0 = u_0(x_p), \quad \forall p \in \mathcal{M}, \quad (2.16)$$

$$u_\sigma^0 = u_0(x_\sigma), \quad \forall \sigma \in \mathcal{E}, \quad (2.17)$$

$$r_p^{n+1} = \int_{n\tau}^{(n+1)\tau} \int_p r(x, t) dx dt, \quad \forall p \in \mathcal{M}, \quad \forall n \in \mathbb{N}, \quad (2.18)$$

$$u_\sigma^{n+1} = 0, \quad \forall \sigma \in \mathcal{E}_{\text{ext}}, \quad \forall n \in \mathbb{N} \quad (2.19)$$

and

$$\begin{aligned} & \frac{|p|}{\tau f_1(N_p(u^n))} (u_p^{n+1} - u_p^n) - \frac{1}{f(N_p(u^n))} \sum_{\sigma \in \mathcal{E}_p} g_{\mathcal{D}}^S \frac{|\sigma|}{d_{p\sigma}} (u_\sigma^{n+1} - u_p^{n+1}) = \\ & = \frac{r_p^{n+1}}{\tau f_1(N_p(u^n))}, \quad \forall p \in \mathcal{M}, \quad \forall n \in \mathbb{N}, \end{aligned} \quad (2.20)$$

where the following relation is given for the interior edges (balance of the fluxes, see (2.6)):

$$g_{\mathcal{D}}^S \frac{u_\sigma^{n+1} - u_p^{n+1}}{f(N_p(u^n)) d_{p\sigma}} + g_{\mathcal{D}}^S \frac{u_\sigma^{n+1} - u_q^{n+1}}{f(N_q(u^n)) d_{q\sigma}} = 0, \quad (2.21)$$

$\forall n \in \mathbb{N}, \forall \sigma \in \mathcal{E}_{\text{int}}$ (the set of interior interfaces) where σ is the edge between p and q .

For the **(APR1)** equation (2.21) turns to the form:

$$\frac{u_\sigma^{n+1} - u_p^{n+1}}{f(N_p(u^n)) d_{p\sigma}} + \frac{u_\sigma^{n+1} - u_q^{n+1}}{f(N_q(u^n)) d_{q\sigma}} = 0 \quad (2.22)$$

and for the **(APR2)** case (2.21) has to be considered in the form:

$$g_p^S \frac{u_\sigma^{n+1} - u_p^{n+1}}{f(N_p(u^n)) d_{p\sigma}} + g_q^S \frac{u_\sigma^{n+1} - u_q^{n+1}}{f(N_q(u^n)) d_{q\sigma}} = 0. \quad (2.23)$$

2.3 Numerical analysis of regularised Riemannian mean curvature flow model

Per its name is this section dedicated to the numerical analysis of the studied model, see [29]. As the first the stability estimates were proven. The L^∞ stability of the scheme estimate:

$$|u_p^n| \leq |u_0|_{\mathcal{D}, \infty} + |r|_{\mathcal{D}, \tau, \infty} n \tau \leq |u_0|_{\mathcal{D}, \infty} + |r|_{\mathcal{D}, \tau, \infty} T, \quad \forall p \in \mathcal{M}, \quad \forall n = 0, \dots, N_T. \quad (2.24)$$

The straightforward implication of (2.24) is the uniqueness of the numerical solution.

Second proven inequality shows $L^2(\Omega \times (0, T))$ estimate on the numerical solution time derivation and $L^\infty(0, T; H_{\mathcal{D}})$ estimate on the numerical solution itself:

$$\begin{aligned} & \frac{1}{2b} \sum_{n=0}^{m-1} \tau \sum_{p \in \mathcal{M}} |p| \left(\frac{u_p^{n+1} - u_p^n}{\tau} \right)^2 + \nu_S \sum_{p \in \mathcal{M}} |p| F(N_p(u^m)) + \\ & + \frac{\nu_S}{2b} \sum_{n=0}^{m-1} \sum_{p \in \mathcal{M}} |p| (N_p(u^{n+1}) - N_p(u^n))^2 \leq \frac{C_\theta \|u^0\|_{H^1(\Omega)}^2 + \|r\|_{L^2(\Omega \times (0, T))}^2}{2a}, \quad \forall m = 1, \dots, N_T. \end{aligned} \quad (2.25)$$

This estimate holds unconditionally for the approximation of the smoothing term $g_{\mathcal{D}}^S$ by **(APR2)**. For the **(APR1)** case the space and the time step have to be of the same order and a constant C depending only on the data of the problem has to be added on the right side of the inequality (2.25). We use above mentioned estimates and another lemmas to prove following theorem, which guarantees the convergence of the scheme (2.20)-(2.21) to the weak solution of the problem (2.7)-(2.8)-(2.9).

Convergence of the semi-implicit FVM scheme to the weak solution of the regularised Riemannian curvature flow equation theorem:

Let the Hypothesis (H) holds and let for all $m \in \mathbb{N}$ be the function $u_{\mathcal{D}_m, \tau_m}$ defined as $u_{\mathcal{D}_m, \tau_m}(x, t) = u_p^{n+1}$ for a.e. $x \in p, \forall t \in (n\tau, (n+1)\tau], \forall p \in \mathcal{M}, \forall n \in \mathbb{N}$. Let $(\mathcal{D}_m, \tau_m)_{m \in \mathbb{N}}$ be the extracted subsequence of the space-time discretisations such that $h_{\mathcal{D}_m}$ and τ_m converge to 0 for $m \rightarrow \infty$.

Then there exists a function $\bar{u} \in L^\infty(0, T; H_0^1(\Omega))$, such that $u_{\mathcal{D}_m, \tau_m} \rightarrow \bar{u}$ in $L^2(0, T; H_0^1(\Omega))$ and this

\bar{u} is the weak solution of (2.7)-(2.8)-(2.9) in the sense of the Definition 2.1. Moreover if we define:

$$\hat{G}_{\mathcal{D},\tau}(x,t) = \frac{1}{|p|} \sum_{\sigma \in \mathcal{E}_p} (u_\sigma^{n+1} - u_p^{n+1})n_{p\sigma}, \quad (2.26)$$

for a.e. $x \in p$, $t \in (n\tau, (n+1)\tau]$, $\forall p \in \mathcal{M}$, $\forall n \in \mathbb{N}$, it holds that $\hat{G}_{\mathcal{D}_m,\tau_m} \rightarrow \nabla \bar{u}$ in $L^2(\Omega \times (0,T))^d$ and $N_{\mathcal{D},\tau}(x,t) \rightarrow |\nabla \bar{u}|$ in $L^2(\Omega \times (0,T))$, where N is defined by (2.13).

2.4 Numerical experiments in image segmentation

To demonstrate advantages of our approach we test the model on the benchmark examples - we chose object with incomplete border and noisy object as examples of the most often appearing errors in the initial data, noise and missing boundaries of the objects, see [28] or [30]:

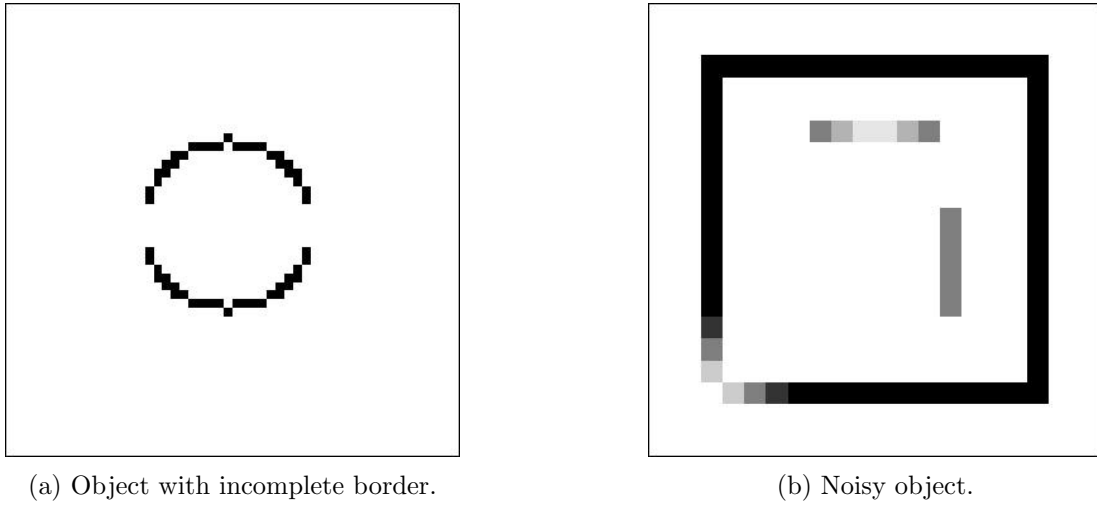


Figure 2.2: Benchmark examples.

As we are using the method based on the level set approach we have to create the initial level set function as the first step. We will monitor the development of the chosen segmented object by monitoring the development of the level set function, better say its isolines. The crucial aspect of this process is that we monitor progress of the whole surface, not just a particular curve, therefore we are able to easily follow the topological changes.

We can see how the situation is looking at the beginning of the segmentation on the following pictures:

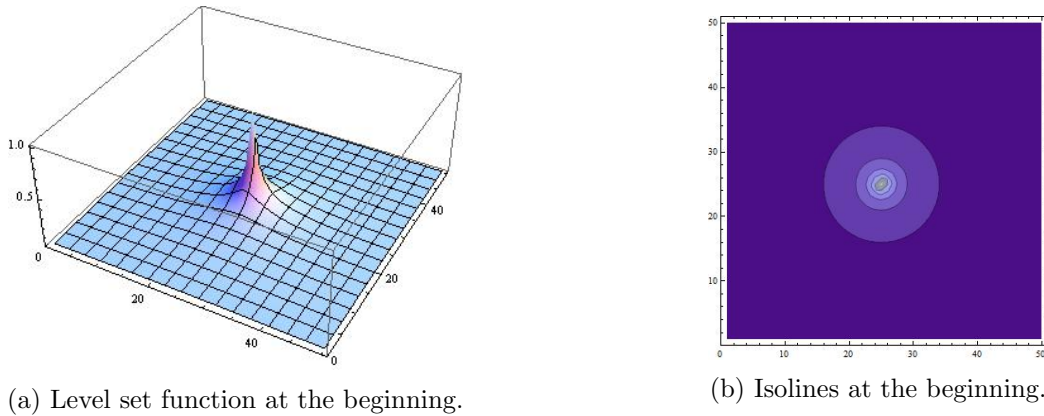


Figure 2.3: Situation at the beginning of the segmentation.

Level set function movement is driven by the curvature, monitored area (it has yellow color on the

picture below and it is the inside of the segmented object) is growing, her borders are pulled to the borders of the segmented object by the constructed vector field.

Constructed scheme based on the level set approach has shown to be robust against the selected errors in the initial data and it is able to segment given objects:

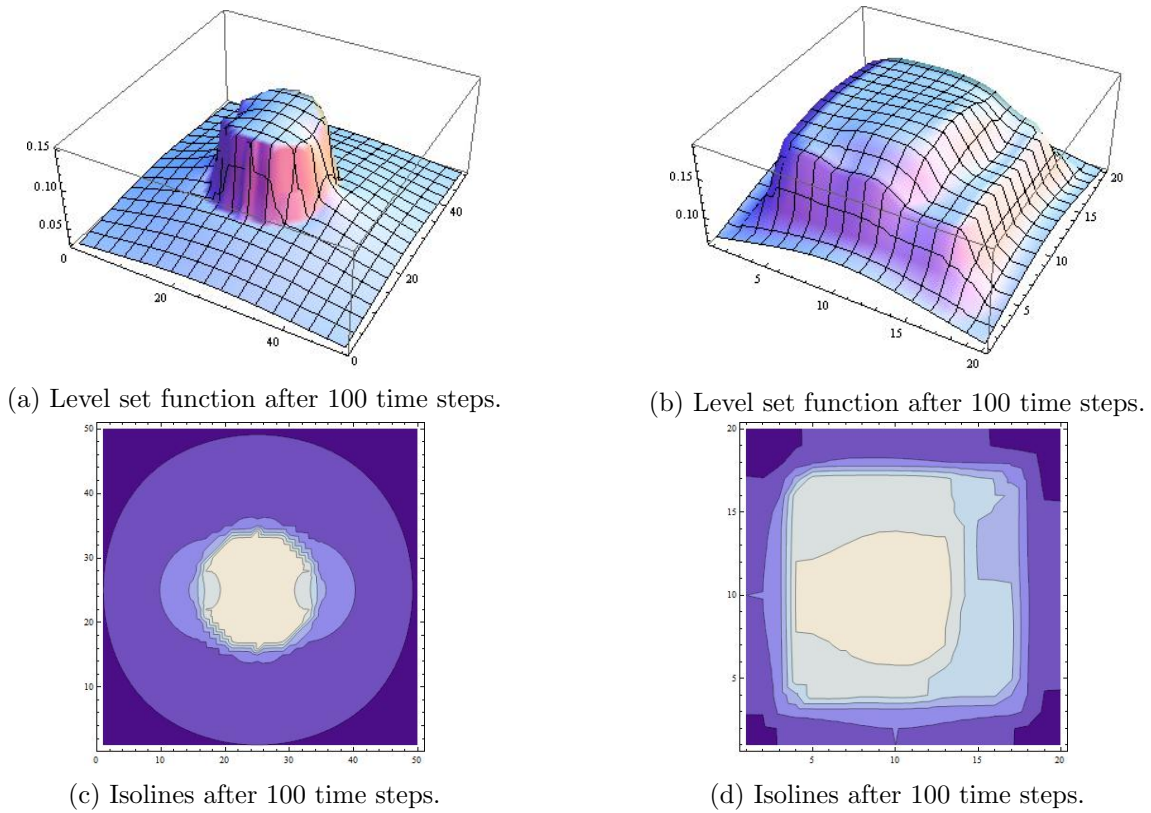


Figure 2.4: Segmentation of the chosen objects.

Second type of the numerical experiment we are presenting is the non-linear smoothing term approximation impact analysis, see [31]. We can see minimal impact from both, visual and numerical, perspectives as demonstrated in the Table 2.1:

Absolute difference after	1 step	10 steps	100 steps	1000 steps
L_1 norm	0.00612	0.13982	0.22316	0.29966
L_2 norm	0.00001	0.00004	0.00013	0.00009
L_∞ norm	0.00086	0.00244	0.00309	0.00098
Relative difference after	1 step	10 steps	100 steps	1000 steps
L_1 norm	0.00039	0.00091	0.00151	0.00098
L_2 norm	7.53e-08	2.78e-07	8.79e-07	7.20e-07
L_∞ norm	5.53e-06	1.59e-05	2.09e-05	7.44e-06

Table 2.1: Absolute and relative norms for sensitivity constant $K = 1$.

The approach (**APR2**) seems to be the better one from the two studied, because the scheme with the approximation (**APR2**) has better theoretical properties (unconditional stability and convergence) and it is easier to implement and because (**APR1**) is better only insignificantly from numerical perspective.

Chapter 3

Gradient Schemes in Financial Derivatives Pricing Problems

We pay attention on the application of the parabolic partial differential equations in the financial derivatives pricing in the second part of the thesis and we solve chosen problem from this problematic using the DDFV numerical method.

3.1 Mathematical models and numerical method in financial mathematics

The idea of financial derivatives is quite straightforward - the price of the derivative depends on the time and on the price of the underlying asset (stock, bond, interest rate, etc.). This gives the investor an opportunity to create a portfolio from underlying assets and their derivatives to avoid risk of potential loss (at least in theory), so-called hedging.

The ground stone of an option pricing - Black-Scholes equation (see [3]):

$$\frac{\partial V}{\partial t} + rS \frac{\partial V}{\partial S} + \frac{1}{2} \sigma^2 S^2 \frac{\partial^2 V}{\partial S^2} - rV = 0. \quad (3.1)$$

was proposed based on the Ito's lemma (see [18] or [19]), the principle of hedging and the assumptions of an idealized financial market:

- (i) trading takes place continuously in time;
- (ii) there are no arbitrage opportunities (no possibility to make riskless profit);
- (iii) the riskless interest rate r is known and constant over time;
- (iv) no transaction costs exist in buying or selling the asset or the option (frictionless market);
- (v) the assets are perfectly divisible and short-selling is permitted;
- (vi) the stock price follows geometric Brownian motion with constant drift and volatility: $dS = \mu S dt + \sigma S dw$, where w is standard Wiener process, see [27];
- (vii) the stock pays no dividend.

As the assumptions of an idealized financial market were found to be too simplifying for the real market conditions a lot of generalisations of the original linear model were developed. Many of them were focused on the assumption (vi), especially to eliminate the the constant volatility of the Brown motion that models the stock price assumption.

Following stochastic differential equation was proposed in [5] to imitate the behaviour of risk-free interest rate:

$$dv_t = \kappa(\theta - v_t)dt + \sigma\sqrt{v_t}dz_t. \quad (3.2)$$

This idea was taken to be the model of the financial derivative volatility development by Heston in [17], which led to the so-called Heston differential equations stated here in its usual form:

$$\frac{\partial V}{\partial t} + \frac{1}{2}vS^2\frac{\partial^2 V}{\partial S^2} + \rho\sigma Sv\frac{\partial^2 V}{\partial S\partial v} + \frac{1}{2}v\sigma^2\frac{\partial^2 V}{\partial v^2} + rS\frac{\partial V}{\partial S} + [\kappa(\theta - v) - \lambda v]\frac{\partial V}{\partial v} - rV = 0. \quad (3.3)$$

After the substitution $x = \ln(\frac{S}{E}), y = v, \tau = T - t, u(x, y, \tau) = \frac{V(S, v, t)}{E}$ the (3.3) can be expressed in the compact form

$$\frac{\partial u}{\partial \tau} + \vec{A} \cdot \nabla u = \nabla \cdot (\mathbf{B}\nabla u) - ru. \quad (3.4)$$

Regularisation of (3.4) together with appropriate initial and boundary conditions constitutes the problem we are studying in this part of our work.

We are using the discrete duality finite volume method (DDFV) for numerical solution. The principle of the DDFV is that we create so-called dual mesh on the top of the original one. In other words there is another triplet $\bar{\mathcal{D}} = (\bar{\mathcal{M}}, \bar{\mathcal{E}}, \bar{\mathcal{P}})$ with the same meaning as explained in the Section 2.1.

On the Figure 3.1 taken from [20] we can see the example for the rectangular square mesh - on the top of the primal (red) mesh there is a dual (black) mesh created.

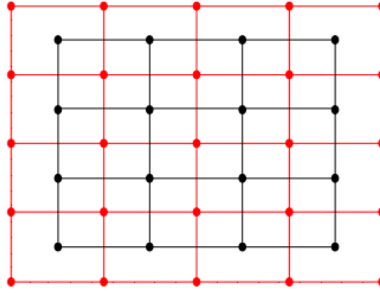


Figure 3.1: Primal (red) and dual (black) mesh.

The crucial advantage which this approach brings from numerical perspective is that, as for rectangular square mesh one can see above on the Figure 3.1, vertexes of the original mesh are points of the dual mesh and vice versa. This feature is very convenient especially for approximation of the flux (represented by gradient in our case) through the boundary of the control volumes.

This is the overall principle of the DDFV derived from the FVM as it is the way we have followed in our study of these numerical methods. The DDFV was firstly used by Andreianov, Boyer, Hubert in [1] and by Domelevo, Omnes in [6].

3.2 Regularised Heston model

We consider following problem: find an unknown function $u = u(x, y, \tau)$ - approximate solution to the equation

$$\frac{\partial u}{\partial \tau} + \vec{A} \cdot \nabla u = \varepsilon\Delta u + \nabla \cdot (\mathbf{B}\nabla u) - ru + f(x, y, \tau), \quad (x, y, \tau) \in \Omega \times [t_1, t_2], \quad (3.5)$$

where $\Omega = (X_a, X_b) \times (0, Y)$ is a rectangular domain and

$$f(x, y, \tau) = \begin{cases} 0 & \text{for } x < -r\tau, \\ \varepsilon e^x & \text{for } x \geq -r\tau. \end{cases} \quad (3.6)$$

The unknown function u fulfils homogeneous initial and boundary conditions, ε is regularisation parameter of the problem and

$$B = \frac{1}{2}y \begin{pmatrix} 1 & \rho\sigma \\ \rho\sigma & \sigma^2 \end{pmatrix}, \vec{A} = - \begin{pmatrix} r - \frac{1}{2}y - \frac{1}{2}\rho\sigma \\ \kappa(\theta - y) - \lambda y - \frac{1}{2}\sigma^2 \end{pmatrix}. \quad (3.7)$$

Based on the boundary condition we divide Γ , boundary of the domain Ω , into two parts such that

$$\Gamma = \Gamma_D \cup \Gamma_N,$$

where $\Gamma_D = \{(x, y) \in \Gamma : x = X_a \vee x = X_b\}$, part of the Γ where Dirichlet boundary conditions are prescribed and $\Gamma_N = \{(x, y) \in \Gamma : y = 0 \vee y = Y\}$, part of the Γ where Neumann boundary conditions are prescribed.

Parameters of the model (3.5) have following meaning and values:

- $\rho \in \langle -1, 1 \rangle$ is the correlation parameter between underlying asset price and the volatility of the financial derivative;
- $\sigma > 0$ is the volatility variance, which is taken to be a stochastic variable as stated in (3.2);
- $\theta > 0$ is the long term variance, around which the financial derivative volatility oscillate;
- $\kappa > 0$ is the reversion speed of the financial derivative volatility return to the long term variance;
- $r > 0$ is the interest rate;
- $\lambda > 0$ is the market price of risk, which models the risk impact.

In analogy to the first part we define weak solution of the problem we are studying. At this point we are following the approach given in [10].

Definition 3.1 (Weak solution of (3.5)) We say that u is a weak solution of (3.5) if, for all $I = \langle t_1, t_2 \rangle$, $0 < t_1 < t_2 < \infty$,

1. $u \in L^2(I; V(\Omega))$, where $V(\Omega) := \{u \in H^1(\Omega) : u|_{\Gamma_D} = 0\}$.
2. $u(\cdot, 0) = 0$.
3. Following holds

$$\begin{aligned} & \int_I \int_{\Omega} -u(x, y, \tau) \frac{\partial \psi}{\partial \tau}(x, y, \tau) + \vec{A} \cdot \nabla u(x, y, \tau) \psi(x, y, \tau) + \varepsilon \nabla u(x, y, \tau) \nabla \psi(x, y, \tau) + \\ & + \mathbf{B} \nabla u(x, y, \tau) \nabla \psi(x, y, \tau) + ru(x, y, \tau) \psi(x, y, \tau) dx dy d\tau = \\ & = \int_I \int_{\Omega} f(x, y, \tau) \psi(x, y, \tau) dx dy d\tau, \\ & \forall \psi \in \mathcal{A} := \{\varphi \in C^1(I; C^1(\Omega)) : \varphi(t_2, \cdot) = 0 \wedge \varphi|_{\Gamma_D} = 0\}. \end{aligned} \quad (3.8)$$

Following the approach presented in [14] and in [15] we can discretize the problem by the fully implicit DDFV numerical scheme.

Under the symbol u_{ij}^n we mean the piecewise constant approximation of the solution in the points of the primal mesh, in analogy \bar{u}_{ij}^n is the approximation on the dual mesh. The numerical solution is then defined as the average of the solution on the primal and dual mesh, similarly for the numerical solution time derivation approximation. We are using the diamond cell method for the numerical solution gradient approximation. We construct the admissible mesh such that h_x is the space step in the direction x and h_y in the direction y . Once we set the diffusion tensor B elements and the convection term \vec{A} elements on the common edge of the control volume p and the control volume q as

$$B_{ij}^{pq} = \begin{pmatrix} b_{ij,pq}^{11} & b_{ij,pq}^{12} \\ b_{ij,pq}^{21} & b_{ij,pq}^{22} \end{pmatrix}, \vec{A}_{ij}^{pq} = \begin{pmatrix} a_{ij,pq}^1 \\ a_{ij,pq}^2 \end{pmatrix} \quad (3.9)$$

we get the scheme for the values u_{ij}^n on the primal mesh

$$\begin{aligned}
& \frac{u_{ij}^n - u_{ij}^{n-1}}{k} h_x h_y - \varepsilon (h_y [u_x^{ij,n} - u_x^{i-1j,n}] + h_x [\bar{u}_y^{ij,n} - \bar{u}_y^{ij-1,n}]) - \\
& - h_y [b_{ij,10}^{11} u_x^{ij,n} + b_{ij,10}^{12} u_y^{ij,n}] - h_x [b_{ij,01}^{21} \bar{u}_x^{ij,n} + b_{ij,01}^{22} \bar{u}_y^{ij,n}] + \\
& + h_y [b_{ij,-10}^{11} u_x^{i-1j,n} + b_{ij,-10}^{12} u_y^{i-1j,n}] + h_x [b_{ij,0-1}^{21} \bar{u}_x^{ij-1,n} + b_{ij,0-1}^{22} \bar{u}_y^{ij-1,n}] + \\
& + h_y a_{ij,10}^1 \frac{u_{i+1j}^n - u_{ij}^n}{2} + h_x a_{ij,01}^2 \frac{u_{ij+1}^n - u_{ij}^n}{2} - h_y a_{ij,-10}^1 \frac{u_{i-1j}^n - u_{ij}^n}{2} - h_x a_{ij,0-1}^2 \frac{u_{ij-1}^n - u_{ij}^n}{2} \\
& + r u_{ij}^n h_x h_y = f_{ij}^n h_x h_y
\end{aligned} \tag{3.10}$$

and for the values \bar{u}_{ij} on the dual mesh

$$\begin{aligned}
& \frac{\bar{u}_{ij}^n - \bar{u}_{ij}^{n-1}}{k} h_x h_y - \varepsilon (h_y [\bar{u}_x^{i+1j,n} - \bar{u}_x^{ij,n}] + h_x [u_y^{ij+1,n} - u_y^{ij,n}]) - \\
& - h_y [b_{i+1j+1,0-1}^{11} \bar{u}_x^{i+1j,n} + b_{i+1j+1,0-1}^{12} \bar{u}_y^{i+1j,n}] - h_x [b_{i+1j+1,-10}^{21} u_x^{ij+1,n} + b_{i+1j+1,-10}^{22} u_y^{ij+1,n}] \\
& + h_y [b_{ij,01}^{11} \bar{u}_x^{ij,n} + b_{ij,01}^{12} \bar{u}_y^{ij,n}] + h_x [b_{ij,11}^{21} u_x^{ij,n} + b_{ij,10}^{22} u_y^{ij,n}] + h_y a_{i+1j+1,0-1}^1 \frac{\bar{u}_{i+1j}^n - \bar{u}_{ij}^n}{2} + \\
& + h_x a_{i+1j+1,-10}^2 \frac{\bar{u}_{ij+1}^n - \bar{u}_{ij}^n}{2} - h_y a_{ij,01}^1 \frac{\bar{u}_{i-1j}^n - \bar{u}_{ij}^n}{2} - h_x a_{ij,10}^2 \frac{\bar{u}_{ij-1}^n - \bar{u}_{ij}^n}{2} \\
& + r \bar{u}_{ij}^n h_x h_y = \bar{f}_{ij}^n h_x h_y.
\end{aligned} \tag{3.11}$$

Properties of these schemes are studied in the next two sections in the terms of their stability and accuracy.

3.3 Numerical analysis of regularised Heston model

We proved the stability estimate on the numerical solution and its gradient in analogy to the first part:

$$\begin{aligned}
& \|u_{k,h}\|_{L_\infty(I;L_2(\Omega))} \leq C, \\
& \|\nabla u_{k,h}\|_{L_2(I;L_2(\Omega))}^2 \leq C(\varepsilon),
\end{aligned} \tag{3.12}$$

where $C(\varepsilon)$ is generic constant depending only on the data of the problem and the regularisation parameter ε , not on parameters k (time step), h_x and h_y (space steps).

Estimate (3.12) helped us prove following theorem stating the convergence of the scheme (3.10) - (3.11) to the weak solution of the problem (3.5).

Convergence of the fully implicit DDFV scheme to the weak solution of the regularised Heston model theorem:

Let Ω be the rectangular domain and $I = [t_1, t_2]$ be the time interval, $0 < t_1 < t_2 < \infty$. Let $u_{k,h}$ be the solution of (3.10) - (3.11). Let (k_m, h_m) be the sequence of the space-time discretisations such that $k_m \rightarrow 0$ and $h_m \rightarrow 0$ for $m \rightarrow \infty$. Then there exists a function $\tilde{u} \in L^2(I; H^1(\Omega))$ such that $u_{k_m, h_m} \rightharpoonup \tilde{u}$ in $L^2(I; H^1(\Omega))$ for $m \rightarrow \infty$ and this \tilde{u} is the weak solution of (3.5) in the sense of the Definition 3.1.

3.4 Numerical experiments in financial derivatives pricing

There are two types of the numerical experiments performed in the financial mathematics part of the work. The first one is focused on the quantification of the regularisation parameter ε impact as the term $\varepsilon \Delta u$ was added to the original Heston model for the numerical analysis purposes only.

One can find L_2 errors of the tested models - classic Heston model (D) and regularised Heston model (R) solved using the DDFV approach for various values of the parameter ε and number of the time steps N_{ts} and the space steps N_x and N_y in the Table 3.1:

N_x	N_y	N_{ts}	L_2D	$L_2R, \varepsilon = 10^{-2}$	$L_2R, \varepsilon = 10^{-4}$	$L_2R, \varepsilon = 10^{-6}$
20	10	1	0.00815061	0.00827543	0.00815181	0.00815063
40	20	4	0.00607821	0.00613972	0.00607879	0.00607822
80	40	16	0.00548663	0.00553226	0.00548706	0.00548664
160	80	64	0.00529716	0.00533972	0.00529756	0.00529716

Table 3.1: Classic and regularised DDFV scheme errors comparison.

The experiment conclusion is that errors of both models are decreasing with the increasing number of the time and space steps. In addition one can see that $L_2R(\varepsilon) \rightarrow L_2D$ as $\varepsilon \rightarrow 0$ for all listed meshes and for ε sufficiently small are the results for the regularised model almost the same as for the non-regularised case.

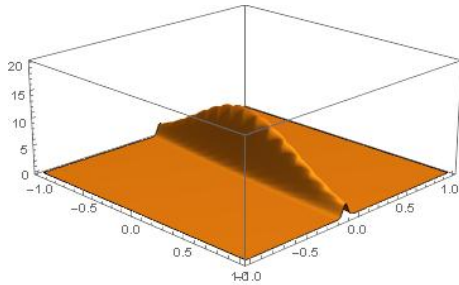
In the second experiment we are solving one phenomenon for the tensor diffusion problems occurring for the model:

$$\frac{\partial u}{\partial \tau} = \nabla \cdot (\mathbf{B} \nabla u), \quad (\mathbf{x}, \tau) \in \Omega \times [t_1, t_2] \quad (3.13)$$

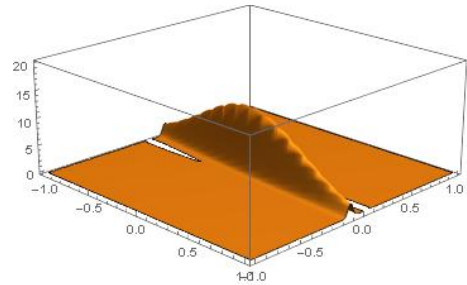
with the known shape of the exact solution, see [22]:

$$u(\mathbf{x}, \tau) = \frac{1}{4\pi\tau\sqrt{|\mathbf{B}|}} e^{-\frac{\mathbf{x}^T \mathbf{B}^{-1} \mathbf{x}}{4\tau}}, \quad (x, y) \in \Omega \subset \mathbb{R}^2, \quad \tau \in [t_1, t_2], \quad t_1, t_2 \in \mathbb{R}, t_2 > t_1 > 0. \quad (3.14)$$

This solution is positive on whole space domain $\Omega = \langle -1; 1 \rangle \times \langle -1; 1 \rangle$ and in the time interval $\langle 0.2; 0.3 \rangle$ as seen on the Figure 3.2. Here one can observe that there are stripes where the solution is negative occurring around axis $y = 0$, when solving this problem numerically with the FVM or the DDFV approach:



(a) Shape of the exact solution.



(b) Shape of the DDFV numerical solution without regularisation.

Figure 3.2: Exact solution negativity zones problem.

There was a regularisation analogical to the one used by us for the Heston model proposed in [15] to solve this issue:

$$\frac{\partial u}{\partial \tau} = \nabla \cdot ((\mathbf{B} + \varepsilon) \nabla u), \quad (\mathbf{x}, \tau) \in \Omega \times [t_1, t_2]. \quad (3.15)$$

In opposite to this global regularisation (on the whole domain Ω) we suggested the local regularisation only on the problematic area around axis $y = 0$, therefore is the model as follows:

$$\frac{\partial u}{\partial \tau} = \nabla \cdot (\mathbf{B}_\varepsilon \nabla u), \quad (\mathbf{x}, \tau) \in \Omega \times [t_1, t_2], \quad (3.16)$$

where \mathbf{B}_ε is defined as

$$\mathbf{B}_\varepsilon(x, y) = \begin{cases} B + \varepsilon, & \text{pre } (x, y) \in \Omega_\varepsilon := \{(x, y) : |y| < \varepsilon\}, \\ B, & \text{pre } (x, y) \in \Omega - \Omega_\varepsilon. \end{cases} \quad (3.17)$$

On the top of the classic L_2 error we are monitoring two new metrics developed for this experiment only - the first one is percentage of the area, where is the corresponding solution negative and the second one is the solution maximum value. We state these metrics values for $N_x = N_y = 160$ and $N_{ts} = 640$ for the exact solution (Exact), model without any regularisation (C), model with the global regularisation (RG) and model with the local regularisation (RL) in the Table 3.2:

metrics	Exact	C	RG, $\varepsilon = 10^{-3}$	RG, $\varepsilon = 10^{-5}$	RL, $\varepsilon = 10^{-3}$	RL, $\varepsilon = 10^{-3}$
percentage	0	1.598	0.262	1.582	0.832	1.578
maximum	12.0919	12.2543	10.5565	12.2333	11.6292	12.247

Table 3.2: Diffusion model experiment tracked metrics.

Only the regularisations with the parameter value $\varepsilon = 10^{-3}$ make sense for the negativeness problem as seen above. The global regularisation achieved better results in this case, but has a problem with the error of the solution maximum approximation. Local regularisation can be interesting and useful compromise with the stated metrics balancing from this perspective.

REFERENCES

- [1] Andreianov B., Boyer F., Hubert F.: Discrete Duality Finite Volume Schemes for Leray-Lions Type Problems on General 2D Meshes, Numerical Methods for PDEs, Vol. 2, No. 1, 145-195, 2007.
- [2] Bertolazzi E., Manzini. G.: On vertex reconstructions for cell-centered finite volume approximations of 2D anisotropic diffusion problems, Mathematical Models and Methods in Applied Sciences, 17(1):1-32, 2007.
- [3] Black F., Scholes M.: The pricing of options and corporate liabilities, The Journal of Political Economy 81, 3, 637-654, 1973.
- [4] Coudiere Y., Manzini. G.: The discrete duality finite volume method for convection-diffusion problems, SIAM Journal on Numerical Analysis, 47(6):4163-4192, 2010.
- [5] Cox J., Ingersoll J., Ross S.: A Theory of the Term Structure of Interest Rates. In: Econometrica 53, 385-407, 1985.
- [6] Domelevo K., Omnes P.: Finite volume method for the Laplace equation on almost arbitrary two-dimensional grids, M2AN, Vol. 39 No 6, 1203-1240, 2013.
- [7] Drbliková O., Komorníková M., Remešíková M., Bourguine P., Mikula K., Peyrieras N., Sarti A.: Estimate of the cell number growth rate using PDE methods of image processing and time series analysis, Journal of Electrical Engineering, Vol. 58, No 7/s, 86-92, 2007.
- [8] Droniou J., Eymard R., Gallouet T., Guichard C., Herbin R.: The gradient discretisation method: A framework for the discretisation and numerical analysis of linear and nonlinear elliptic and parabolic problems, 2016. hal-01382358v3
- [9] Evans L. C., Spruck J.: Motion of level sets by mean curvature, J, Diff, Geom., 33(3):635-681, 1991.
- [10] Eymard R., Gallouet T., Herbin R.: Finite Volume Method, Handbook of Numerical Analysis, Vol. VII, 713-1020, 2000.
- [11] Eymard R., Handlovičová A., Herbin R., Mikula K., Stašová O.: Applications of approximate gradient schemes for nonlinear parabolic equations, Applications of Mathematics, Vol. 60, No. 2, 135-156, 2015.
- [12] Eymard R., Handlovičová A., Mikula K.: Non-diffusive numerical scheme for regularized mean curvature flow level set equation in image processing, Proceedings of the 3rd International Congress on Image and Signal Processing CISP-BMEI 2010, Yantai, China, Vol. 2, 748-753, 2010.
- [13] Eymard R., Handlovičová A., Mikula K.: Study of a finite volume scheme for regularised mean curvature flow level set equation, IMA Journal on Numerical Analysis, Vol. 31, 813-846, 2011.

- [14] Handlovičová A.: Discrete duality finite volume scheme for solving Heston model, Proceedings of ALGORITMY 264-274, 2016.
- [15] Handlovičová A.: Stability estimates for discrete duality finite volume scheme for Heston model, Computer Methods in Materials Science, 17, 101-110, 2017.
- [16] Handlovičová A., Mikula K., Sgallari F.: Semi-implicit complementary volume scheme for solving level set like equations in image processing and curve evolution, Numer. Math., 93(4):675-695, 2003.
- [17] Heston, S. L.: A Closed-Form Solution for Options with Stochastic Volatility with Applications to Bond and Currency Options. In: The Review of Financial Studies 6, 2, 327-343, 1993, ISSN: 0893-9454.
- [18] Ito K.: Stochastic integral, Proc. Imp. Acad., Vol 20., No. 8, 519-524, 1944.
- [19] Ito K.: On Stochastic Differential Equations, Memoris Of The American Mathematical Society, No. 4, 1-51, 1951.
- [20] Kotorová D.: Discrete Duality Finite Volume Scheme for the Curvature-driven Level Set Equation, Acta Polytechnica Hungarica, Vol. 8, No. 3, 2011.
- [21] Krivá Z., Handlovičová A., Mikula K.: Adaptive cell-centered finite volume method for diffusion equations on a consistent quadtree grid, Advances in Computational Mathematics, Vol. 42, No. 2, 249-277, 2016. <https://doi.org/10.1007/s10444-015-9423-2>.
- [22] Kútik P.: Numerical solution of partial differential equations and their application, Dissertation Thesis, Slovak University of Technology, 2013.
- [23] Mikula K., Krivá Z., Stašová O.: Spracovanie obrazu, scriptum, STU, 2016.
- [24] Osher S., Sethian J. A.: Fronts propagating with curvature-dependent speed: Algorithms based on Hamilton-Jacobi formulations, J. Comput. Phys., 79(1): 12-49, 1988.
- [25] Perona P., Malik J.: Scale-space and edge detection using anisotropic diffusion, In. Proc. IEEE Computer Society Workshop on Computer Vision, 16-22, 1987.
- [26] Perona P., Malik J.: Scale-space and edge detection using anisotropic diffusion, IEEE Trans. Pattern Anal. Mach. Intell., 629-639, 1990.
- [27] Ševčovič D., Stehlíková B., Mikula M.: Analytical and numerical methods for pricing financial derivatives. Hauppauge, NY: Nova Science Publishers, 2011. ISBN: 978-1-61728-780-0.
- [28] Tibenský M., Handlovičová A.: Application of the mean curvature flow in the image segmentation, In Differential Equations and Applications: book of abstracts, September, 2017, Brno, Czech Republic. 1. vyd. Brno : Institute of Mathematics, Faculty of Mechanical Engineering, Brno University of Technology, s. 77, 2017.
- [29] Tibenský M., Handlovičová A.: Convergence of the numerical scheme for regularised Riemannian mean curvature flow equation, Tatra Mountains Mathematical Publications, accepted, 2018.
- [30] Tibenský M., Handlovičová A.: Numerical scheme for regularised Riemannian mean curvature flow equation, In CANCES, C. – OMNES, P, Finite Volumes for Complex Applications VIII - Methods and Theoretical Aspects: proceedings. FVCA 8, Lille, France, June 2017, Berlin : Springer, 2017, s. 411–419. ISBN 978-3-319-57396-0.
- [31] Tibenský M., Handlovičová A.: Two approaches for the approximation of the nonlinear smoothing term in the image segmentation, Proceedings Of Equadiff 2017 Conference, 229-236, 2017.